*R*esearch in
*A*stronomy and
*A*strophysics

LETTERS

A possible explanation of the Maunder minimum from a flux transport dynamo model

Arnab Rai Choudhuri and Bidya Binay Karak

Department of Physics, Indian Institute of Science, Bangalore-560012, India;
arnab@physics.iisc.ernet.in

Abstract We propose that the poloidal field at the end of the last sunspot cycle before the Maunder minimum fell to a very low value due to fluctuations in the Babcock–Leighton process. With this assumption, a flux transport dynamo model is able to explain various aspects of the historical records of the Maunder minimum remarkably well by suitably choosing the parameters of the model to give the correct growth time.

Key words: Sun: activity — Sun: magnetic fields — sunspots

1 INTRODUCTION

One of the most remarkable features of sunspot activity is the Maunder minimum—a period during 1645 – 1715 when very few sunspots were seen. Since sunspot activity has been unexpectedly low for more than a year now, questions are being raised whether we are on the threshold of another such grand minimum. The sunspot cycle is produced by the dynamo process in the Sun. It is important to understand the possible physical mechanism which could have pushed the dynamo into the Maunder minimum.

Several authors have studied the archival records of sunspots during the Maunder minimum (Sokoloff & Nesme-Ribes 1994; Hoyt & Schatten 1996). The few sunspots seen during the Maunder minimum mostly appeared in the southern hemisphere. Sokoloff & Nesme-Ribes (1994) have used the archival data to construct a butterfly diagram for a part of the Maunder minimum from 1670. Usoskin, Mursula & Kovaltsov (2000) argue that the Maunder minimum started abruptly but ended in a gradual manner, indicating that the strength of the dynamo must be building up as the Sun came out of the Maunder minimum. When solar activity is stronger, magnetic fields in the solar wind suppress the cosmic ray flux, reducing the production of ^{10}Be and ^{14}C which can be used as proxies for solar activity. From the analysis of ^{10}Be abundance in a polar ice core, Beer, Tobias & Weiss (1998) concluded that the solar activity cycle continued during the Maunder minimum, although the overall level of the activity was lower than usual. Miyahara et al. (2004) drew the same conclusion from their analysis of ^{14}C abundance in tree rings.

Beer, Tobias & Weiss (1998) suggested that the nonlinearities in an interface dynamo could be the cause of the Maunder minimum. The flux transport dynamo, in which the poloidal field is produced near the solar surface by the Babcock–Lieghton mechanism and transport by meridional circulation plays an important role, has emerged as an attractive model for the solar cycle ever since the first two-dimensional models were constructed by Choudhuri, Schüssler & Dikpati (1995) and Durney (1995). Our aim is to explore whether the Maunder minimum can be explained within the framework of the flux transport dynamo model developed by our group (Nandy & Choudhuri 2002; Chatterjee, Nandy & Choudhuri 2004).

It is not yet established whether the irregularities in the solar cycle are caused primarily by the nonlinearities (Beer, Tobias & Weiss 1998) or by stochastic fluctuations (Choudhuri 1992; Brandenburg & Spiegel 2008). Charbonneau, Blais-Laurier & St-Jean (2004) presented flux transport dynamo simulations with stochastic fluctuations, which led to intermittencies resembling the Maunder minimum. These simulations used a rather low turbulent diffusivity of 1.67×10^{11} cm^2 s^{-1}. Such a low diffusivity makes the diffusive decay time or the 'memory' of the dynamo very long (on the order of a century) and most probably this long memory played a role in producing intermittencies of similar duration. As argued by Jiang, Chatterjee & Choudhuri (2007), there are several compelling reasons to believe that the diffusivity is at least one order of magnitude larger, making the memory not longer than a few years. We explore whether such a short-memory flux transport dynamo can give rise to the Maunder minimum.

After discussing the methodology in Section 2, we present the results in Section 3. Our main conclusions are summarized in Section 4.

2 METHODOLOGY

Choudhuri, Chatterjee & Jiang (2007) argue that the Babcock–Leighton mechanism, in which the poloidal field is produced from the decay of tilted bipolar sunspots, involves randomness because the convective buffeting on rising flux tubes causes a scatter in the tilt angles (Longcope & Choudhuri 2002). The simplest way of treating this randomness is to introduce a fluctuation in the poloidal field produced at the end of a cycle. Although the statistics may not yet be completely convincing, there is evidence that the polar field at the end of a cycle has a correlation with the strength of the next cycle. Jiang, Chatterjee & Choudhuri (2007, see also Yeates, Nandy & Mackay 2008) showed that a flux transport dynamo model with a reasonably high turbulent diffusivity can explain this correlation. This observed correlation suggests that the polar field at the end of the last cycle just before the Maunder minimum might have been very low. We present a calculation based on this assumption.

In spite of the fluctuations in the Babcock–Leighton process, one may wonder if there is a statistically significant probability of the polar field falling to a very low value at the end of a cycle. Right now, we are carrying on a detailed analysis of that. It is known that a large bipolar sunspot pair can produce a very large perturbation in the Babcock–Leighton process (Wang, Nash & Sheeley 1989). During the decay phase of a cycle, if a very large bipolar sunspot pair emerges with a 'wrong' tilt (i.e. with the following spot closer to the equator), it may be possible for it to neutralize the polar field which had been growing due to contributions from the earlier spots. Even if such a thing happens in one hemisphere, it would seem to be extremely improbable for this to happen in the two hemispheres simultaneously. In the flux transport dynamo with a reasonably high diffusivity, however, the two hemispheres remain coupled and the growth of large hemispheric asymmetries are suppressed due to this diffusive coupling (Chatterjee & Choudhuri 2006; Goel & Choudhuri 2009). Observational data also suggest that hemispheric asymmetries have never been very large in the cycles during the last century (Goel & Choudhuri 2009). So, if the polar field approaches zero in one hemisphere, it is possible that diffusive coupling will also make it small in the other hemisphere. Representing the dynamo by a simple iterative map, Charbonneau (2005) also concluded that a strong cross-hemispheric coupling was essential for the production of the Maunder minimum.

We present calculations on the basis of the ansatz that the polar field at the end of the last cycle before the Maunder minimum fell to a rather low value in the northern hemisphere (like 0.1 of the typical average value of the polar field at the end of a cycle) and also became quite low in the southern hemisphere due to the diffusive coupling between the hemispheres. We do not try to justify this ansatz further in this paper. A future paper will analyze this ansatz further and will try to estimate a statistical probability of such a thing happening. Here, we merely show that this ansatz allows the flux transport dynamo model to reproduce many features of the Maunder minimum remarkably well.

3 RESULTS

We carry out our calculations with the solar dynamo code *Surya*, which is made available upon request. The details of our dynamo model can be found in Chatterjee, Nandy & Choudhuri (2004). It

was suggested by Choudhuri, Chatterjee & Jiang (2007) that the cumulative effect of fluctuations in the Babcock–Leighton process during the decaying phase of a cycle can be modelled by stopping the dynamo code at the end of a sunspot cycle and then multiplying the poloidal field function $A(r, \theta)$ above $r = 0.8\,R_\odot$ by a factor γ. Goel & Choudhuri (2009) used two values of γ for the two hemispheres in order to model the hemispheric asymmetry. Following this approach, we stop the code at a sunspot minimum after obtaining a relaxed periodic solution. Then, in the northern hemisphere, we multiply $A(r, \theta)$ above $r = 0.8\,R_\odot$ by a factor γ_N, whereas we use the factor γ_S for the southern hemisphere. To get good results, we have to make another assumption which we agree is somewhat ad hoc. One of the unsatisfactory aspects of our model so far is that we have been unable to avoid some degree of overlap between cycles (i.e. the previous cycle continues at low latitudes even after the new cycle has started at high latitudes). See figure 13 of Chatterjee, Nandy & Choudhuri (2004) or figure 3 of Choudhuri, Chatterjee & Jiang (2007). Although one also sees some amount of overlap between cycles in the observational data, our theoretical model has a much bigger overlap. Since we do not want further eruptions to take place and produce more poloidal field after we have set the poloidal field to low values, we multiply the toroidal field $B(r, \theta)$ everywhere by a factor $\gamma_t = 0.8$ at the same time that we change the poloidal field. As a sunspot eruption in our model takes place only when B is above a critical value B_c, this reduction in B ensures that an eruption will not take place for some time.

After stopping the code at a sunspot minimum and making these changes, we run the code for several cycles without any further interruption. When we choose the same parameters as Choudhuri, Chatterjee & Jiang (2007), we find that the dynamo, which had the poloidal field reduced to very low values at a minimum, bounces back to its original strength in a growth time of about 35 yr. In the case of a simple $\alpha\Omega$ dynamo, it can be analytically shown that the growth time is prolonged by decreasing α or increasing the diffusivity η (see, for example, Choudhuri 1998, sect. 16.6). The same seems to hold for the more complex flux transport dynamo as well. We find that we get an appropriate growth time if we reduce the amplitude of α from $25\,\mathrm{m\,s^{-1}}$ to $21\,\mathrm{m\,s^{-1}}$ and increase the turbulent diffusivity η_p of the poloidal field within the convection zone from $2.4 \times 10^{12}\,\mathrm{cm^2\,s^{-1}}$ to $3.2 \times 10^{12}\,\mathrm{cm^2\,s^{-1}}$. With these values of α and η_p, we use the poloidal field reduction factors $\gamma_N = 0.0$ and $\gamma_S = 0.4$ at a minimum. Figure 1(a) shows the theoretical butterfly diagram, whereas Figure 1(b) shows the sunspot number as a function of time. In order to facilitate comparison with observational data, we have taken the beginning of Figure 1 to be the year 1640. Hopefully, all readers will agree that these two figures are remarkably similar to the observational butterfly diagram given in figure 1(a) of Sokoloff & Nesme-Ribes (1994) and the observational sunspot number plot given in figure 1 of Usoskin, Mursula & Kovaltsov (2000).

Even though the diffusive decay time or the memory of our dynamo is only a few years, it is possible to get a grand minimum of much longer duration by making the growth time suitably large. The indication in the observational data that solar activity at the beginning of the Maunder minimum decreased abruptly and then built up gradually (Usoskin, Mursula & Kovaltsov 2000) strongly supports our interpretation that a grand minimum is caused by a sudden decrease in the poloidal field due to fluctuations in the Babcock–Leighton process and then the dynamo regains its strength during its growth time. If the duration of the grand minimum is really an indication of the dynamo growth time, then it is possible to put constraints on the parameters of the dynamo from this. The combination of parameters we used to produce Figure 1 is by no means the only combination that gives the correct duration of the grand minimum. Table 1 lists some other combinations which also produce grand minima resembling the Maunder minimum. It may be noted that α/η_p^2 for all these combinations are comparable, suggesting that the dynamo numbers (see, for example, Choudhuri 1998, sect. 16.6) for these combinations are comparable.

Sunspots do not erupt in our model until the toroidal field builds up to a strength larger than B_c. Even when there are few or no sunspots, the dynamo must be growing in an oscillatory fashion. In the absence of sunspots, the Babcock–Leighton process is not possible. As argued by Choudhuri (2003), the toroidal field is expected to be concentrated in limited regions outside of which it may be diffuse. Since flux tube simulations (Choudhuri 1989; D'Silva & Choudhuri 1993; Fan, Fisher & DeLuca 1993) suggest that the initial field strength inside flux tubes has to be of order $10^5\,\mathrm{G}$, an eruption presumably takes place only when the concentrated field reaches a value of $10^5\,\mathrm{G}$ (corresponding to B_c in our model).
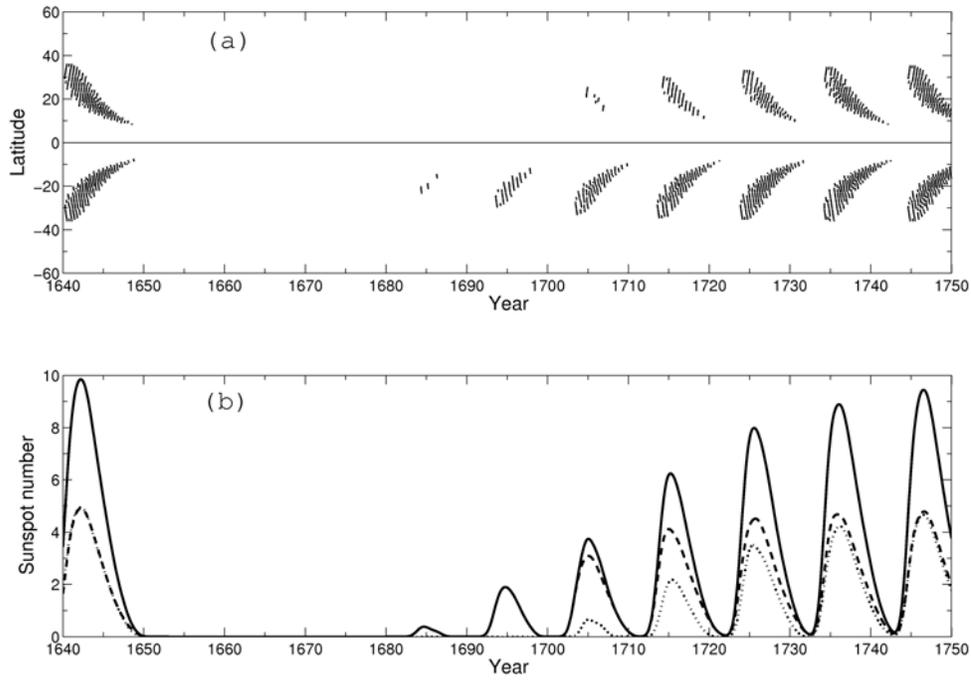
Fig. 1 Theoretical results from our dynamo simulation covering the Maunder minimum. (a) The theoretical butterfly diagram. (b) The theoretical sunspot number (this is obtained by first considering the monthly number of eruptions and then smoothing it by iteratively taking a running average over 5 months). The dashed and dotted lines show the sunspot numbers in the northern and southern hemispheres, whereas the solid line is the total sunspot number.

Table 1 A Few Combinations of Parameters which Produce Figures Similar to Fig. 1

η_p (cm^2 s^{-1})	α(m s^{-1})	α/η_p^2	γ_t	γ_N	γ_S
3.2×10^{12}	21	2.05×10^{-24}	0.8	0.0	0.4
3.2×10^{12}	20	1.95×10^{-24}	0.8	0.2	0.6
			0.9	0.0	0.4
3.3×10^{12}	22	2.02×10^{-24}	0.8	0.2	0.6
			0.9	0.0	0.5
2.9×10^{12}	17	2.02×10^{-24}	0.8	0.2	0.6
			0.9	0.0	0.4
2.7×10^{12}	15	2.06×10^{-24}	0.8	0.2	0.6
			0.9	0.0	0.5
2.2×10^{12}	11	2.27×10^{-24}	0.8	0.2	0.6
			0.9	0.0	0.4

If the toroidal field does not become strong enough to produce sunspot eruptions, then presumably this toroidal field is carried upward in the low-latitude regions of the convection zone by the upflowing meridional circulation (and probably also the uprising regions of convection). The α coefficient in our equations acting on this toroidal field can be interpreted as the traditional α in mean field MHD (see Choudhuri 1998, sect. 16.5). Even when sunspot eruptions take place, Choudhuri & Dikpati (1999) concluded that the distribution of large-scale solar magnetic field can be modeled particularly well by assuming the poloidal field to have two sources—from the Babcock–Leighton mechanism and from the α effect working on the weaker subsurface toroidal field. When sunspots are absent, the strength of the dynamo builds up due to the α effect operating on the weaker toroidal field.

The ^{10}Be and ^{14}C abundances depend on the magnetic field in the solar wind. We have implemented the upper boundary condition in our model in such a way that the magnetic field becomes radial beyond a distance of $3\,R_\odot$ due to the stretching by the solar wind (see Dikpati & Choudhuri 1995). At a distance where the magnetic field is radial, its average strength can be obtained by averaging over the spherical surface there, i.e.

$$\langle |B_r(r)| \rangle = \frac{1}{2} \int_0^\pi |B_r(r,\theta)| \sin\theta \, d\theta.$$

Figure 2 shows this as a function of time; the sudden change around 1648 being due to the change in the poloidal field. Although the strength of $\langle |B_r(r)| \rangle$ becomes weaker during the Maunder minimum, the oscillations in the magnetic field continue, explaining why oscillations are seen in the ^{10}Be and ^{14}C abundance data during the Maunder minimum. It is interesting to note that the magnetic field in the solar wind in our model does not become that much weaker even when there are no sunspots.
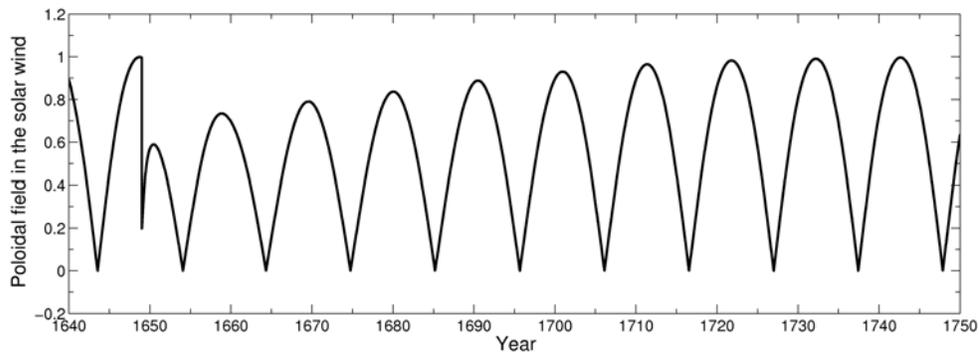

Fig. 2 Theoretically calculated average radial magnetic field in the solar wind (in arbitrary units) as a function of time.

4 CONCLUSIONS

We have shown that different characteristics of the Maunder minimum can be explained very elegantly on the basis of the simple ansatz that, as a result of randomness in the Babcock–Leighton process, the poloidal field at the end of the last cycle before the Maunder minimum fell to a rather low value in the northern hemisphere and also became small in the southern hemisphere due to the diffusive coupling between the hemispheres. While we are carrying on an analysis to show that this ansatz can be justified on statistical grounds, the fact that calculations based on this ansatz agree with observational data so extremely well gives credence to this ansatz. Our model explains why the Maunder minimum started abruptly, but ended with a more gradual growth of cycle strengths. In the case of the 'failed' Dalton minimum (cycles 5 and 6) also, sunspot number data indicate that the cycle strength fell abruptly and

then grew more gradually. The growth time in this case was shorter than what it was in the case of the Maunder minimum. While we are identifying the duration of the Maunder minimum with the dynamo growth time, it should be kept in mind that this is not a linear problem. The toroidal field is not allowed to grow much beyond B_c due to magnetic buoyancy. If the fall in dynamo strength is less abrupt, then the dynamo bounces back in a shorter time. Even to produce the Maunder minimum in our model, we did not have to use unreasonably low polar field diminution factors at the end of a cycle ($\gamma_N = 0.0$ and $\gamma_S = 0.4$ being our choices).

We end with a comment on whether we could be entering another grand minimum right now. Based on the polar field data provided by Svalgaard, Cliver & Kamide (2005), Choudhuri, Chatterjee & Jiang (2007) estimated that the polar field diminution factor γ at the end of cycle 23 was 0.6. According to our dynamo model, this drop in the polar field is not sufficient to cause a grand minimum without sunspot eruptions for many years. However, in view of the various uncertainties in our model, we should keep our mind open and wait to see what the Sun has in store for us.

References

Beer, J., Tobias, S., & Weiss, N. 1998, Solar Phys., 181, 237

Brandenburg, A., & Spiegel, E. A. 2008, AN, 329, 351

Charbonneau, P. 2005, Solar Phys., 229, 345

Charbonneau, P., Blais-Laurier, G., & St-Jean, C. 2004, ApJ, 616, L183

Chatterjee, P., & Choudhuri, A. R. 2006, Solar Phys., 239, 29

Chatterjee, P., Nandy, D., & Choudhuri, A. R. 2004, A&A, 427, 1019

Choudhuri, A. R. 1989, Solar Phys., 123, 217

Choudhuri, A. R. 1992, A&A, 253, 277

Choudhuri, A. R. 1998, The Physics of Fluids and Plasmas: An Introduction for Astrophysicists (Cambridge: Cambridge University Press)

Choudhuri, A. R. 2003, Solar Phys., 215, 31

Choudhuri, A. R., Chatterjee, P., & Jiang, J. 2007, Phys. Rev. Lett., 98, 131103

Choudhuri, A. R., & Dikpati, M. 1999, Solar Phys., 184, 61

Choudhuri, A. R., Schüssler, M., & Dikpati, M. 1995, A&A, 303, L29

D'Silva, S., & Choudhuri, A. R. 1993, A&A, 272, 621

Dikpati, M., & Choudhuri, A. R. 1995, Solar Phys., 161, 9

Durney, B. R. 1995, Solar Phys., 160, 213

Fan, Y., Fisher, G. H., & DeLuca, E. E. 1993, ApJ, 405, 390

Goel, A., & Choudhuri, A. R. 2009, RAA (Research Astron. Astrophys.), 9, 115

Hoyt, D. V., & Schatten, K. H. 1996, Solar Phy., 165, 181

Jiang, J., Chatterjee, P., & Choudhuri, A. R. 2007, MNRAS, 381, 1527

Longcope, D., & Choudhuri, A. R. 2002, Solar Phys., 205, 63

Miyahara, H., Masuda, K., Muraki, Y., Furuzawa, H., Menjo, H., & Nakamura, T. 2004, Solar Phys., 224, 317

Nandy, D., & Choudhuri, A. R. 2002, Science, 296, 1671

Sokoloff, D., & Nesme-Ribes, E. 1994, A&A, 288, 293

Svalgaard, L., Cliver, E. W., & Kamide, Y. 2005, Geo. Res. Lett., 32, L01104

Usoskin, I. G., Mursula, K., & Kovaltsov, G. A. 2000, A&A, 354, L33

Wang, Y.-M., Nash, A. G., & Sheeley, N. R. 1989, ApJ, 347, 529

Yeates, A. R., Nandy, D., & Mackay, D. H. 2008, ApJ, 673, 544